Simulating the Dynamics of a Chain Suspended Sub-sea Load Using Modified Components from the Modelica MultiBody Library

Savin Viswanathan[1] Christian Holden[1]

[1]Dept. of Mechanical and Industrial Engineering, Norwegian University of Science and Technology (NTNU), NO-7491 Trondheim, Norway. {savin.viswanathan,christian.holden}@ntnu.no

Abstract

In this paper, the philosophy of the lumped-mass approach is adopted in specifying *components* so as to enable the *Modelica* compiler to formulate equations governing the motion of a chain-suspended sub-sea load, subjected to waves and current. The *discretized* simulation model of the chain-suspended load is built up using the components available in the *MultiBody* library of *OpenModelica*, after making necessary modifications. The combined wave and current loads acting on the segments are determined using the Morison equation, and applied as discrete external forces on the lumped segmental masses. The component model is developed and implemented using the *OMEdit* GUI, and the simulation results are then compared with those for a similar system modelled in the popular commercial ocean-engineering time-domain simulation software, *Orcaflex*, to demonstrate satisfactory agreement. Conclusions are drawn, and the simulation files are made available for public access.

Keywords: Modelica component-model for submerged cables, dynamics of sub-sea loads, OceanEngineering library

1 Introduction

The authors discussed the benefits of developing a *Modelica* standard library for ocean-engineering applications in (Viswanathan and Holden, 2019). In the above work, the *quasi-static* approach was adopted to specify the mooring forces at any given simulation time-step. However, it was noted that this led to the omission of the inertial and deflection effects of the mooring line, as discussed in detail by the authors in (Viswanathan and Holden, 2020a). Hence, steps in the direction of developing component-models capable of simulating the dynamic behaviour of mooring chains, as accurately as possible, were adopted by the authors. The present work, which is an offshoot of such efforts, brings to the *proposed* library, basic components to simulate the dynamics of a fully submerged, suspended sub-sea load.

The earliest reference to the application of the *lumped-mass* approach to sub-sea cables is traced to Walton *et. al* (Walton and Polachek, 1960), who prescribes the lumping of masses of straight segment lengths, and associated external forces, at nodal points which connect the adjoining segments, and thus arrive at equations of motions for the *discretized* mathematical model of the physically *continuous* cable. They further suggest a fixed time-step numerical scheme to obtain the cable dynamics. Other relevant works include (Nakajima et al., 1982), and (Thomas and Hearn, 1994).

We, however, notice that such *time-step* dependent methods are inherently opposed to a fundamental philosophy behind *Modelica*, which is expressed by Dr. Michael Tiller in his words, (Tiller, 2013):

"The key point is that equations describing physical behavior cannot refer to time steps. This is because there is no timestep *in nature or the laws of physics, and so the response of a system cannot depend on it."*

The statement points to the fact that the *Modelica* user needs to specify only the differential algebraic equations governing the physics of the system, and solution methodology is best left to the *Modelica* compiler.

We, therefore, adopt the philosophy of Walton in modelling the cable/chain segments in *Modelica*, using components already available in the *Modelica.Mechanics.MultiBody* library, albeit with necessary modifications. Connecting these components enable the automatic generation of the coupled equations of motion by the *Modelica* compiler, which is then solved for obtaining the system dynamics.

The Morison equation is widely used in the ocean engineering domain to calculate fluid loads on slender structures. Numerous publications deal with the subject, and is described in detail, for e.g., in (Chakrabarti, 1987). In this work, the *Morison* equation is implemented as a *Block*, and the determined fluid drag and inertia loads are then applied as forces, along with buoyancy, at the lumped-mass points.

We, therefore, proceed by presenting a brief theoretical introduction to the *discretization* of the *continuous* cable/chain, along with the calculation of Morison loads. This is followed by a detailed description of system representation in *Modelica*. Simulation results are benchmarked using *Orcaflex*, and conclusions drawn. Both *Modelica* and *Orcaflex* simulation files are made available for public access at github.com/Savin-Viswanathan/Modelica2020Asia.

2 Theory

Figure 1a shows the forces acting on a chain suspended sub-sea load, and Figure 1b shows the discretized mathematical model for the same.

For simplicity, we consider:

- 2D motions in x and y directions only.
- Top end of the chain is fixed.
- Inelastic chain.
- Fully submerged chain and load at all times.
- End load has negligible drag area, and can be approximated as a point mass.

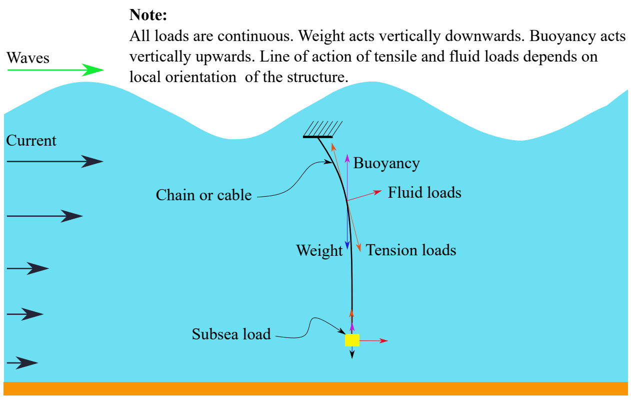

(a) Continuous physical model.

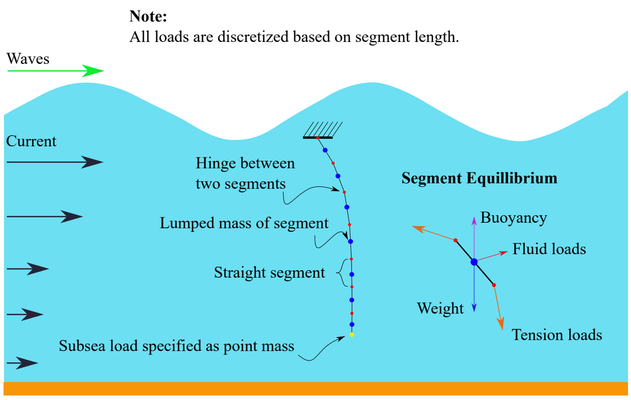

(b) Discretized mathematical model.

Figure 1. Discretization of the chain suspended sub-sea load.

The coupled equations of motion of the chain/cable segments based on the segment equillibrium may then be solved to determine the dynamic behaviour of the system.

Proper translation of the *discretized* model into a *Modelica* system-model effects the automatic generation of the coupled equations of motion governing the dynamic behaviour of the system. Details of modelling are described in detail in the next section.

Considering the j^{th} segment,

$$W_j = l_j \mu g \tag{1}$$

$$B_j = \frac{\pi D_b^2}{4} l_j \rho_w g. \tag{2}$$

Here, W_j [N] is the weight of the segment, B_j [N] is the buoyancy force experienced by the segment, l_j [m] is the length of the segment, μ [kg/m] is the specific linear mass of the chain/cable, D_b [m] is the diameter based on which buoyancy is calculated, ρ_w [kg/m^3] is the density of seawater, and g [m/s^2] is the acceleration due to gravity.

In evaluating the fluid loads, we make use of the Morison equation for combined wave and current loads on an inclined oscillating cylinder. See p. 188 of (Chakrabarti, 1987).

Experimental values for drag coefficient C_D and inertial coefficient C_M are scarce when structures are inclined. Hence, in determining these loads, we evaluate the fluid loads along the normal and tangential directions of the chain segment and then sum up their horizontal and vertical components. The advantage of this approach is that it enables the specification of separate drag (C_D) and inertia (C_M) coefficients for the normal and tangential directions. See p. 205 of (Chakrabarti, 1987). The normal and tangential components of the Morison force per unit length of the segment are thus given as

$$\begin{aligned} M_F^n =& C_M^n \rho \frac{\pi}{4} D^2 a_w^n - C_A^n \rho \frac{\pi}{4} D^2 a_l^n \\ &+ C_D^n \frac{1}{2} \rho D \mid v_w^n \pm U^n - v_l^n \mid (v_w^n \pm U^n - v_l^n). \end{aligned} \tag{3}$$

$$\begin{aligned} M_F^t =& C_M^t \rho \frac{\pi}{4} D^2 a_w^t - C_A^t \rho \frac{\pi}{4} D^2 a_l^t \\ &+ C_D^t \frac{1}{2} \rho D \mid v_w^t \pm U^t - v_l^t \mid (v_w^t \pm U^t - v_l^t). \end{aligned} \tag{4}$$

Here, superscripts n and t denote the normal and tangential directions, and subscripts w and l denote the water-particle and the mooring-segment respectively. Further, a [m/s^2] refers to acceleration, v refers to velocity, U [m/s] is the magnitude of the current velocity, and D [m] is the line drag diameter.

The current velocity, and wave induced water-particle velocities and accelerations, at the segment lumped-mass points, are to be considered in (3) and (4).

For a linear wave, the following are defined:

$$\omega^2 = gk \tanh(kd) \tag{5}$$

$$\eta = H/2 \cos(kx - \omega t), \tag{6}$$

$$u = \frac{\pi H}{T} \frac{\cosh k(z+d)}{\sinh(kd)} \cos(kx - \omega t) \tag{7}$$

$$w = \frac{\pi H}{T} \frac{\sinh k(z+d)}{\sinh(kd)} \sin(kx - \omega t) \tag{8}$$

$$\dot{u} = \frac{2\pi^2 H}{T^2} \frac{\cosh k(z+d)}{\sinh(kd)} \sin(kx - \omega t) \tag{9}$$

$$\dot{w} = -\frac{2\pi^2 H}{T^2} \frac{\sinh k(z+d)}{\sinh(kd)} \cos(kx - \omega t). \tag{10}$$

DOI 10.3384/ecp2017459

Here, ω [rad/s] is the wave frequency, η [m] is the sea surface elevation, u and w [m/s] are the horizontal and vertical components of the wave-induced water particle velocities, the overdot denotes time derivative, H [m] is the wave height, T [s] is the wave period, k [m^{-1}] is the wave number, x and z [m] are the horizontal and vertical co-ordinates of the evaluation point, d [m] is the water depth, and t [s] is the simulation time. See pp. 51–52 of (Chakrabarti, 1987).

Figure 2 gives the expression for the normal and tangential components of the wave-induced water particle velocities associated with a segment inclined at angle θ to the horizontal. Similar expressions may be obtained for the relevant current, and segment kinematics.

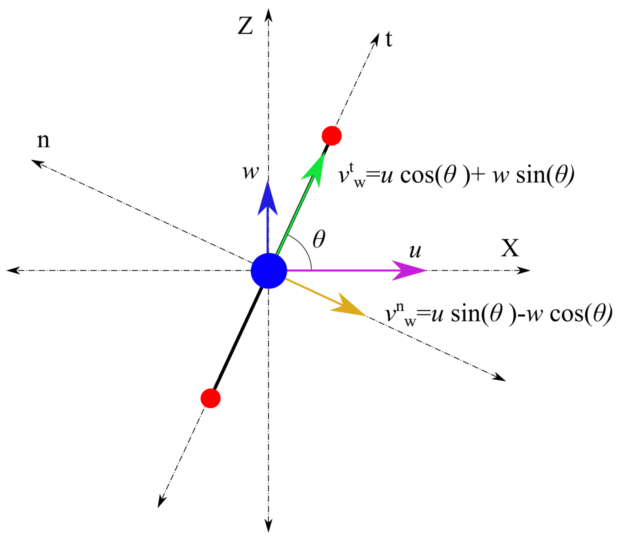

Figure 2. Normal and tangential components.

The horizontal and vertical components of the Morison loads on the segment may thus be determined as:

$$M_F^x = M_F^t \cos\theta + M_F^n \sin\theta \tag{11}$$
$$M_F^y = M_F^t \sin\theta - M_F^n \cos\theta . \tag{12}$$

The problem is implicit in the sense of the interdependency between line orientation, tension and fluid loading.

3 Building the Modelica Model

Representation of the *discretized* model in *Modelica* is realized through the use of components already available in the Multi-Body-System (MBS) library of *Modelica*, with some modifications to meet the problem requirements.

The segmental lumped mass, and the suspended load, are represented by **PointMass** components, the massless lengths of segments lying on either side of its lumped-mass are represented by **FixedTranslation** components, the point of suspension of the top end is specified by a **Fixed** component, and the hinge connection between the segments are represented by **Revolute** joint components, all of which are available in the MBS library.

In the determination of fluid loads, we require the orientation of the segment at any given simulation time step, and hence a modification is effected to the **FixedTranslation** component by specifying a *RealOutput* interface to transmit the coordinates of the flanges. Two variants of the **FixedTranslation** components are specified, the icon representations of which are shown in Figure 3.

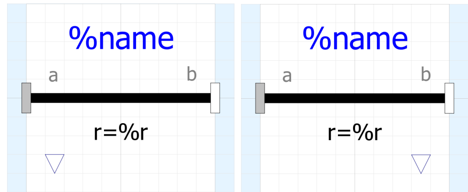

(a) UP_Seg. **(b)** LO_Seg.

Figure 3. *Icon* views of the modified *FixedTranslation* components.

UP_Seg is modified such that its *RealOutput* interface transmits the coordinates of its *flange_a*.

LO_Seg is modified such that its *RealOutput* interface transmits the coordinates of its *flange_b*.

The *diagram view* of the simplest sample system showing all used components is shown in Figure 4.

The segment model is built up by connecting the appropriate flanges of upper segment **UP_Seg**, a **PointMass**, and a lower segment **LO_Seg**. The interconnection between two segments, and of a segment with the point of suspension, can be effected through a **Revolute** joint. The point of suspension of the top end is specified by a **Fixed** component, and a **PointMass** component is used to specify the suspended load. Drag calculations are carried out by **DnB** blocks.The computed drag and buoyancy values are transformed to world forces by a **WorldForce** component, and applied as loads to the flanges of the lumped-masses. Gravity is included by the specification of the **World** component.

The environment, and cable/chain parameters, are specified inside the **DnB** block. The parameters specified are:

General: water depth d, water density ρ, ramping period for waves and current T_{rmp}.

Regular Wave: wave height H, period T.

Current: *vector* of depths at which the profile is defined z_{cg} and fully developed magnitudes of current at these depths U_f.

Cable: drag diameter D, buoyancy diameter D_b, normal and tangential added mass coefficients C_A^n and C_A^t. normal and tangential drag coefficients C_D^n and C_D^t.

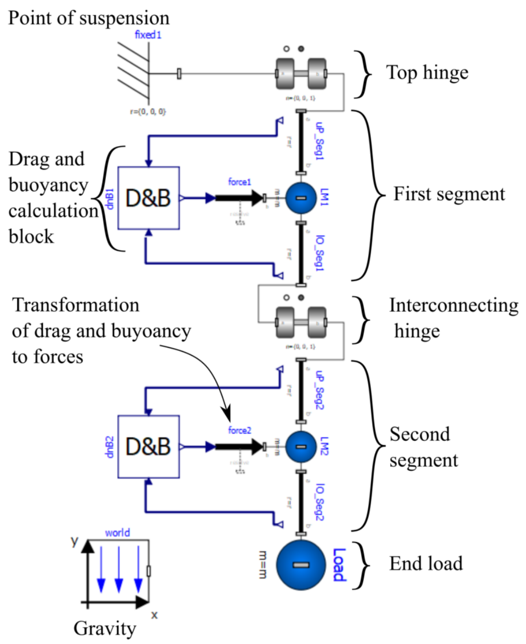

Figure 4. Modelica representation of a suspended subsea load system.

Parameter	**Value**
Depth of suspension point below water surface	2.5 [m]
Chain length	30 [m]
Chain specific mass	10 [kg/m]
Discretization segment length	5 [m]
Chain buoyancy diameter	0.04 [m]
Chain drag diameter	0.04 [m]
Chain drag coeff. (normal)	1 [-]
Chain drag coeff. (tangential)	0.25 [-]
Chain added mass coeff. (normal)	1 [-]
Chain added mass coeff. (tangential)	0.5[-]
End load mass	100 [kg]
Ramp time for waves and current	10 [s]
Water depth	50 [m]
Water density	1025 [kg/m^3]
Current profile	*variable*
Regular wave parameters	*variable*

Table 1. System parameters

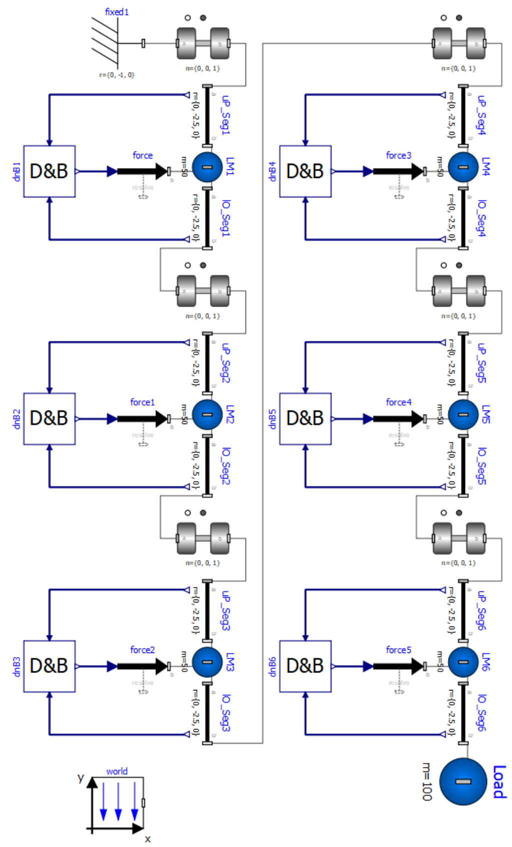

Figure 5. Diagram view of a subsea suspended load *system*.

The wave number is computed by *function* **waveNumberIterator**, by iteration of the dispersion relation (5), as described in (Viswanathan and Holden, 2020b). The segment lengths, and instantaneous location of *lumped-mass* points are calculated based on the real outputs of the **UP_Seg**, and **LO_Seg**, associated with each segment.

The sea surface elevation (SSE) at the x co-ordinate of the *lumped-mass* point is calculated using (6), and the wave and current kinematic profiles are moved with the SSE as described in (SINTEF, 2014). The current velocity at the y coordinate of the *lumped-mass* point is then interpolated for using the **linearInterpolatorSV** *function*, and the wave-induced water-particle velocities and accelerations are calculated using (7)–(10).

The velocities and accelerations of the *lumped-mass* points at the current time step being provided by *Modelica*, the instantaneous drag may be determined using equations (3), (4), (11), and (12).

Drag and buoyancy forces on the end load may also be specified by using a similar **DnB** block, but has been omitted here for simplicity.

4 Results

We discuss the simulation results of a system with parameters shown in Table 1:

Figure 5 shows the diagram view of the above system in *Modelica*.

Figure 6a compares the line configurations in *Modelica* and *Orcaflex*, at $t = 100$ [s], when subject to a uniform current profile defined by $z_{cg} = \{-50, -25, -10, 0\}, U_f = \{1, 1, 1, 1\}$. Figure 6b compares the same for a current profile defined by $z_{cg} = \{-50, -25, -10, 0\}, U_f = \{0, 0.5, 1, 2\}$. In both cases, the wave height $H = 0$ [m].

Figure 7 compares the top end tensions for both the above cases.

Figures 8a and 8b compare the horizontal and vertical response of the suspended load to regular waves of $H = 5$ [m] and $T = 10$ [s], in both *Modelica* and *Orcaflex*, while Figure 8c compares the top end tensions. Current loading is set to zero by specifying $z_{cg} = \{-50, -25, -10, 0\}, U_f = \{0, 0, 0, 0\}$.

DOI 10.3384/ecp2017459

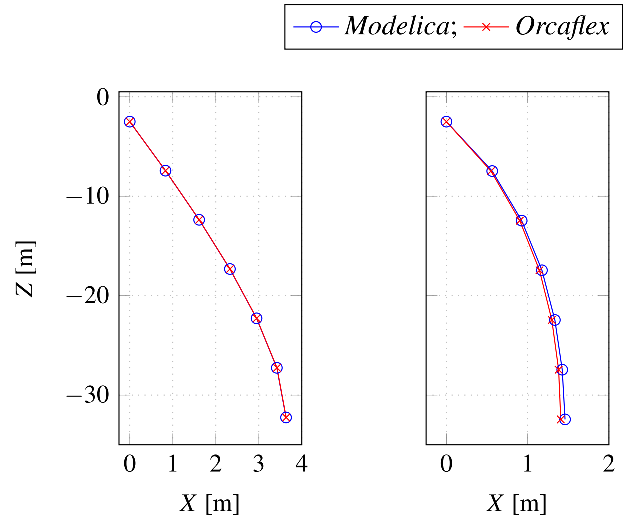

(a) Unifrom profile **(b)** Non-uniform profile

Figure 6. Line configuration for different current profiles.

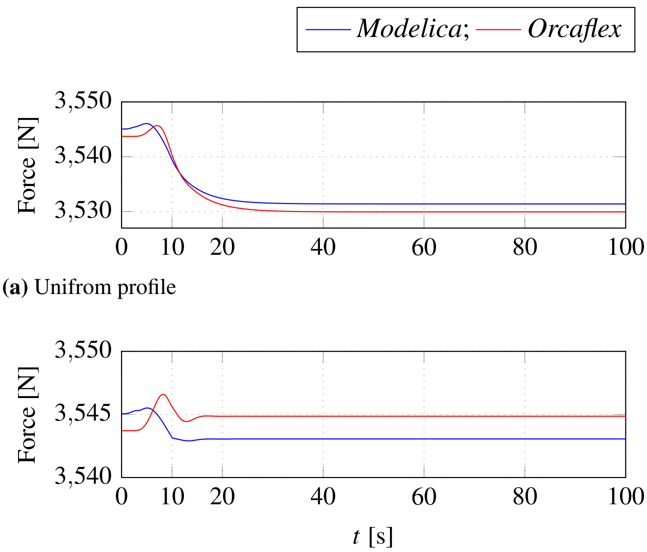

(a) Unifrom profile

(b) Non-uniform profile

Figure 7. Line top end tensions for different current profiles.

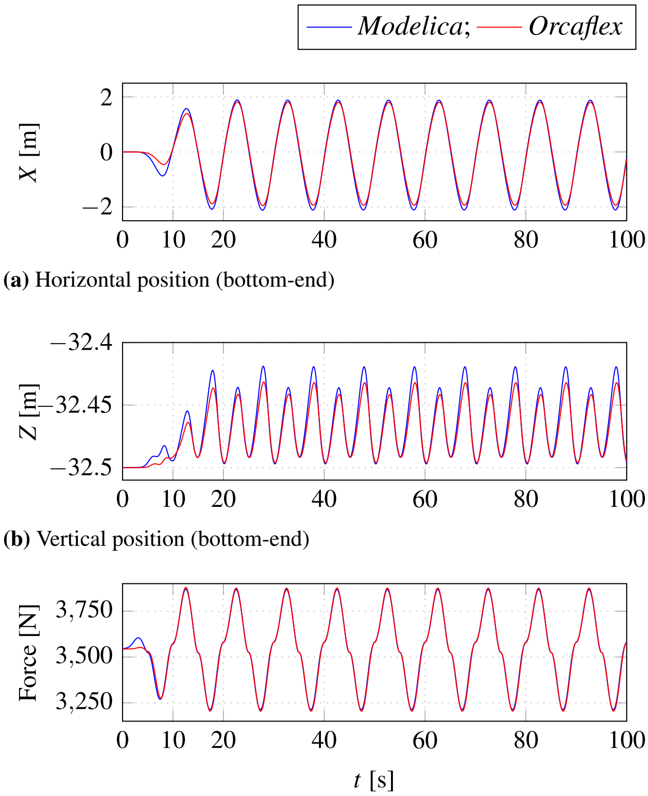

(a) Horizontal position (bottom-end)

(b) Vertical position (bottom-end)

(c) Top end tension

Figure 8. Regular wave response.

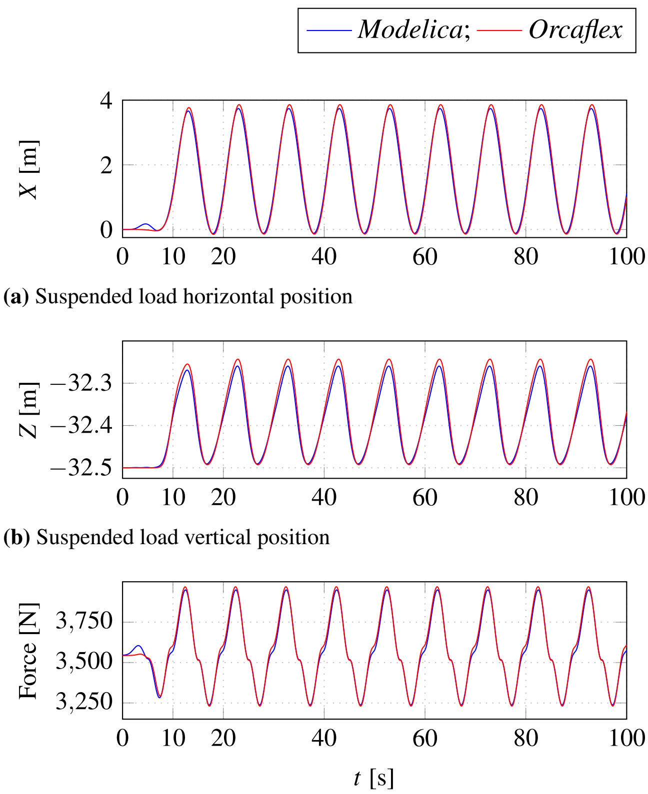

(a) Suspended load horizontal position

(b) Suspended load vertical position

(c) Top end tension

Figure 9. Combined wave–current response.

Figure 9a and Figure 9b compares the horizontal and vertical response of the suspended load to regular waves of $H = 5$ [m] and $T = 10$ [s] in the presence of a current with profile defined by $z_{cg} = \{-50, -25, -10, 0\}, U_f = \{0, 0.5, 1, 2\}$, in both *Modelica* and *Orcaflex*, while Figure 9c compares the top end tensions.

5 Result Discussion

From the above figures, we observe a general agreement between *Modelica* and *Orcaflex* responses. To quantify the degree of agreement, we present the percentage variation between them in Table. 2.

In most cases, we observe good agreement with <5% variation. On examining the values with higher % variation, we infer that the numerical significance is quite low, as demonstrated below for the highest variation of 21.9%, corresponding to the vertical displacement of the suspended load, as depicted in Fig. 8b.

Numerically, the *Modelica* and *Orcaflex* responses are $-32.4193-(-32.4970) = 0.0777$ [m], and $-32.4324-(-32.4960) = 0.0636$ [m], indicating a difference of 0.014 [m], which is quite insignificant when we consider that this variation of 1.4 cm is for the motion of the tip of a chain that is 30 [m] long. Similar inferences can be arrived at for all other values.

These variations could be due to the fact that we use *moved* kinematic profiles, while *Orcaflex* uses *Wheeler stretching* of wave and current kinematics.

Larger variations observed during the ramp-up time $T_{rmp} = 10$ [s], in all cases, is attributed to the fact that we use a sinusoidal ramping function while *Orcaflex* uses an in-built ramping function with a different ramp curve.

The reason for the variation in initial top-end tension and tension response to currents as observed in Figure 7, though insignificant, has not yet been understood.

Variable Description	**%variation**
Horizontal position of end load in uniform current (Fig. 6a)	-0.07
Horizontal position of end load in profile current (Fig. 6b)	3.72
Vertical position of end load in uniform current (Fig. 6a)	0.00
Vertical position of end load in profile current (Fig. 6b)	-0.03
Top end tension in uniform current (Fig. 7a)	0.04
Top end tension in profile current (Fig. 7b)	-0.05
Horizontal response in waves (Fig. 8a)	6.47
Vertical response in waves (Fig. 8b)	21.9
Top end tension response in waves (Fig. 8c)	-2.34
Horizontal response in waves and current (Fig. 9a)	-3.62
Vertical response in waves and current (Fig. 9b)	-7.31
Top end tension response in waves and current (Fig. 9c)	-11.11

Table 2. Variation between *Modelica* and *Orcaflex* results.

6 Conclusion

The work presented in this paper introduces a novel method for specifying fluid loads on a mass discretized subsea cable using components already available in the *Modelica MultiBody* library, with minor modifications.

Based on the agreement between *Modelica* and *Orcaflex* simulation results, it is concluded that the model exhibits satisfactory representation of structural and fluid inertia effects, and accurate modelling of the drag loads on a cable structure.

The only traceable reference to an attempt to use *Modelica* in a similar scenario, by other researchers, is in the modelling of the station keeping system of an offshore wind turbine in (Leimeister and Thomas, 2017), where limitations included the inability to account for:

- Relative accelerations in wave load calculation.
- Current loads on submerged structures.

These limitations have been successfully mitigated in the present model.

It may also be noted that the authors are relatively new to *Modelica*, and the results presented here are for a work in progress. The code presented along with this work may show instances of under-utilization of advantages offered by *Modelica*, for e.g., the use of the *array* concept in implementing the lumped mass philosophy. The main focus of the present stage of the authors' research is to build a general framework for simulation of ocean engineering systems in *Modelica*. Code refinement is planned for the next stage of the project.

Extension of the modelling philosophy presented in this work is expected to open the window towards the development of *Modelica* component models for catenary as well as taut moorings. Inclusion of linear and torsional spring elements is expected to enable *Modelica* representation of flexible structures with elasticity and bending stiffness viz. risers, elastic moorings, and umbilicals, in the future.

The further development of this work, coupled with the development of component models for waves and currents as described in (Viswanathan and Holden, 2020b), and for non-diffracting floating objects as described in (Viswanathan and Holden, 2020a), followed by the development of component models for diffracting objects in the future, would thus enable the integrated simulation of multiphysical ocean-engineering systems, in their entirety, using *Modelica*.

Presently, the authors are developing an *open-source* code for determining the hydrodynamic coefficients which appear in the equation-of-motion of diffracting floating-objects. The initial results look promising, and the subject will be dealt with in a future publication.

7 Acknowledgements

The research in this paper has received funding from the Research Council of Norway, SFI Offshore Mechatronics, project number 90034210.

References

Subratha Kumar Chakrabarti. *Hydrodynamics of Offshore Structures*. Computational Mechanics Publications, and Springer-Verlag, Dorchester, Great Britain, 1987. ISBN 0-905451-66-X.

Mareike Leimeister and Philipp Thomas. The onewind modelica library for floating offshore wind turbine simulations with flexible structures. In *Proceeding of the 12th International Modelica Conference*, pages 633–642, 05 2017. doi:10.3384/ecp17132633.

Toshio Nakajima, Seizo Motora, and Masataka Fujino. On the dynamic analysis of multi-component mooring lines. In *Proceedings of the Offshore Technology Conference*, 1982. doi:10.4043/4309-ms.

SINTEF. *Handbook on Design and Operation of Flexible Pipes*. 2014. URL `sintef.no/en/latest-news/updated-handbook-on-design-and-operation-of-flexible-pipes/`.

D.O Thomas and G.E. Hearn. Deepwater mooring line dynamics with emphasis on seabed interference effects. In *Proceedings of the Offshore Technology Conference*, volume OTC-7488-MS, May 1994. doi:10.4043/7488-MS.

Michael Tiller. Response to questions on determining variable values of previous time steps in modelica. In *Stackoverflow*, 2013. URL `https://stackoverflow.com/questions/16558587/how-to-determine-value-from-previous-time-step-during-simulation-in-modelica`.

Savin Viswanathan and Christian Holden. Towards the development of an ocean engineering library for openmodelica. In *Proceedings of the ASME 2019 38th International Conference on Ocean, Offshore and Arctic Engineering*, volume 7B:Ocean Engineering. OMAE, November 2019. doi:10.1115/OMAE2019-95054.

Savin Viswanathan and Christian Holden. Modelica component-models for non-diffracting floating objects and quasi-static catenary moorings. In *Proceedings of the American Modelica Conference*, 2020a. The conference has been postponed due to the prevailing COVID-19 situation. A link to the referred publication will be provided along with the download files for the referring publication, as and when such a link becomes available.

Savin Viswanathan and Christian Holden. Modelica component-models for oceanic surface-waves and depth varying current. In *Proceedings of the American Modelica Conference*, 2020b. The conference has been postponed due to the prevailing COVID-19 situation. A link to the referred publication will be provided along with the download files for the referring publication, as and when such a link becomes available.

Thomas S. Walton and Harry Polachek. Calculation of transient motion of submerged cables. *Mathematics of Computation*, 14(69):27–46, 1960. doi:10.1090/S0025-5718-1960-0116470-5.